RECENT DEVELOPMENTS IN CFD AT ARA

A J Bocci
Aircraft Research Association Limited
Manton Lane, Bedford, England.

ABSTRACT

The paper discusses recent work in the Theoretical Division at the Aircraft Research Association Limited (ARA) on the modelling of complex configurations, rotors, propulsion and viscous flows. The general features of the ARA multiblock system, which provides a grid generation and Euler flow solution capability for complex configurations, are discussed. Although very successful, the system has various limitations, in particular the tendency for the grid quality to depend on configuration complexity and type. A new multiblock system is being developed which allows regions of unstructured grid to be included, giving increased flexibility in dealing with complex geometries and other improvements. Work on rotors has included the development of a new Euler code for propellers, as a replacement for the code in current use. Improvements in flow solution offered by the new code are illustrated. In the propulsion field, the extension of a viscous-coupled Euler code for afterbody flows to a complete cowl unit is described briefly. The code is particularly relevant to the new generation of large civil turbofans. Work on Navier-Stokes methods for afterbody/nozzle flows is also discussed. Other work on viscous flows includes a 2-D investigation into viscous modelling with hybrid grids, and the further development of an established transonic flow aerofoil code.

NOTATION

c	Aerofoil or wing chord
C_D	Drag coefficient
C_L	Lift coefficient
C_M	Pitching moment coefficient
C_p	Pressure coefficient
C_p^*	Pressure coefficient for $M_L = 1.0$
J	Propeller advance ratio, number of diameters advanced in one revolution
JPR	Jet pressure ratio to free stream value
k	Turbulence kinetic energy
L	Distance to trailing edge of afterbody or propulsion unit.
M	Free stream Mach number
MFR	Mass flow ratio
M_L	Local Mach number
p	Static pressure
R_c	Non-dimensional radius based on propeller blade radius
Re	Reynolds number
V_x	Axial velocity in propeller field
V_θ	Swirl, or circumferential, velocity in propeller field
x	Chordwise distance
α	Incidence to free stream
δ^*	Boundary layer displacement thickness
ε	Turbulence energy dissipation rate
η	Non-dimensional spanwise position on wing based on semi-span

1 INTRODUCTION

A significant contribution to the UK effort in theoretical aerodynamics has been made by the group at ARA over the years. Most of the work has been carried out on behalf of the Royal Aerospace Establishment (RAE), Dowty Rotol Ltd. and British Aerospace plc (BAe). The work has involved both the development of advanced CFD methods and the use of the methods in investigations intended to advance aerodynamic design standards and for general research purposes. Among the notable achievements of the group have been the following:

(a) Development of the ARA Full-Potential method [1] for the inviscid compressible flow about wing/body combinations. This method has been used by BAe as the main aerodynamic design tool for the wings of the Airbus A330/A340 series of aircraft.

(b) Design of the ARA-D propeller blade aerofoil sections[2] and the development of advanced methods for propeller flow prediction[3]. Dowty Rotol propellers with blades featuring ARA-D sections are fitted to a number of operating aircraft, such as the Jetstream 31, Saab 340 and Fokker 50, and the methods developed are made use of by Dowty Rotol for advanced propeller design.

(c) Development of the ARA multiblock system[4] for grid generation and Euler flow solution about complex aircraft configurations. This system is in use within ARA[5], RAE[6] and, in a modified form, within BAe[7].

In addition to the above, there have been substantial developments in other areas such as propulsion modelling and laminar flow/transition prediction. Methods application work includes the design and subsequent wind tunnel test of military and civil aircraft research configurations and helicopter blade aerofoils.

This paper discusses recent developments in CFD at ARA. For this purpose it is convenient to classify the work into the four topic areas of *complex configurations*, *rotors*, *propulsion* and *viscous flows*. The work in each of these areas will be discussed in general terms, bringing out points of particular technical interest.

The work on complex configurations is described in section 2. The main features of the ARA multiblock system, involving a structured grid, are described and then the characteristics of a new hybrid system, involving both structured and unstructured regions of grid, are outlined. The work on rotors is discussed in section 3, concentrating on an improved Euler method for propellers. The propulsion modelling developments are summarised in section 4, including discussion of both viscous-coupled Euler and Navier-Stokes methods. Other work on viscous flows is commented on in section 5, including both investigations of the calculation of such flows using hybrid grids and the improved representation of extensive flow separation by an established transonic flow aerofoil code. An indication of future plans is given in the conclusions.

2 COMPLEX CONFIGURATIONS

Work in this area at ARA commenced around 1978 with an attempt to extend the Full Potential wing/body method[1] to deal with an underwing pylon/nacelle. It was found that the generation of suitable surface and field grids presented considerable difficulties, even for this restricted class of configuration. Consideration of this problem, and other ideas in this rapidly developing field, led to the initiation around 1982 of the development of the ARA multiblock system for the generation of grids about 3-D aircraft configurations. Progress on the work was reported in Ref 8 and an initial version of the system, coupled to an Euler flow solver[9], was released in the UK in 1986, following demonstrations of its ability to deal with various complex configurations, including for example a wing/body/foreplane[4]. Subsequent work has been concentrated on extending the range of configurations with which the system can deal and, recently, on the first stages of developing a more flexible, 'hybrid', system containing regions of unstructured grid embedded within the overall structured grid.

The basis of the multiblock concept is the division of the flow field into non-overlapping blocks, arranged so that body-conforming grids are defined by the node-to-node interface of the grids at the block faces. The grid is generated by a set of elliptic partial differential equations[10] which map a curvilinear coordinate system of points in each block in real space to uniformly spaced points in the three coordinate directions of a cube in computational space. On each face of a block the boundary condition is of a single type. On a solid surface or far field boundary the grid points are specified (Dirichlet type). On a block boundary internal to the field, grid point positions arise from the condition that grid lines should pass smoothly through the block face (Neumann type), imposed using grid points accessed from adjacent blocks.

As an example of a 2-D multiblock grid, consider the case of a C-grid about an aerofoil embedded in an overall Cartesian H-grid. A schematic of the block structure local to the aerofoil is shown in Fig 1(a), with the aerofoil represented by the slit AA', and the corresponding C-grid is shown in Fig 1(b). The grid lines connect points on opposite faces of each block, forming a quasi-orthogonal set. In the outer field the block edges and thus the grid lines are roughly in line with the Cartesian coordinate axes. Local to the aerofoil the grid lines either meet the surface in an approximately normal direction or follow the surface. As indicated in Fig 1(a) the block arrangement at the nose of the aerofoil ensures that the grid lines curve around the nose.

The ARA multiblock system involves implementation of the above concept in 3-D by means of a comprehensive set of computer codes for grid generation, together with an Euler flow solver. A primary objective in the development of the system was to reduce the burden on the user by minimising, as far as possible, the amount of user interaction required. The structure of the system is indicated below. Although well documented elsewhere[4,8,11] it is worth summarising the main features of the system here.

The topology definition involves the arrangement of blocks in the field appropriate to a given configuration, and this is automated to minimise user interaction. The blocks are arranged to give body-conforming grids within a Cartesian structure in the far field. The surface topology is consistent with that of the adjacent field blocks and the surface grid is generated using the 2-D form of the grid generation equations, with boundary points derived from the input geometry. The grid point

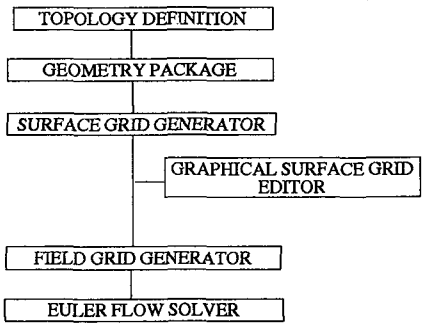

MULTIBLOCK SYSTEM STRUCTURE

distribution on the 3-D far field boundary is set up automatically, with points clustered appropriately about block edges consistent with the distribution on the configuration geometry. The 3-D grid generation equations then define a field grid. The quality of the field grid is highly dependent on the quality of the surface grid and, on occasions, an unsatisfactory grid is derived, which could involve grid crossover or 'negative' cell volumes. It is usually possible to correct such features, and improve the visual quality of the grid, by making use of a graphical surface grid editing facility. Having defined a suitable grid, the solution of the Euler equations over the complete flow field is obtained using the finite-volume, cell-centre algorithm of Jameson et al[12] with, as for the grid generation, a single type of boundary condition applied on each block face. Pre- and post-processing facilities, including graphical means of interrogating the grids and flow solution, are an essential requirement in using all parts of the system.

A 3-D multiblock grid for a wing/body case is shown in Fig 2. The grid structure is apparent from the planes through the field grid. The C-grid which is apparent on the surface of the body adjacent to the wing root is consistent with the field grid around the wing. Due to the arrangement of blocks, singularities of the mapping occur at certain outer corners of the blocks adjacent to the surfaces. Although not presenting serious numerical problems in defining the grid, such singularities can give rise to stretched and distorted cell shapes, as seen in Fig 2 (and also in Fig 1(b)).

The ARA multiblock system has been developed to the stage at which grids and good quality Euler solutions may be obtained for a wide range of complex configurations. To reach this stage the full-time commitment of a team of specialists at ARA has been required over a number of years. As an example of what can be achieved the solution for an advanced military aircraft configuration, with modelling of the intake and exhaust flows, is given in Figs 3(a), (b). The surface grid is shown in Fig 3(a), the field grid being defined by 468 blocks with about 300,000 grid cells. The large number of blocks is typical of complex configurations and presents no fundamental problems, except that the limited number of grid points in each block means that full advantage cannot be taken of computer vectorisation facilities. The flow solution is shown in Fig 3(b) and can be seen to give a good prediction of experimental pressures on the lifting surfaces. It is interesting to note that the predicted foreplane loading varied significantly with intake mass flow in the calculations and this adds to the relevance of such calculations as a complement to wind tunnel testing, where the ability to vary intake mass flow on a typical through-flow model is usually more limited.

Although the multiblock concept is proving very successful, the quality of the grid, or the ability to produce a grid which is satisfactory in all regions of the field, may be very dependent on configuration geometry. For example, it has proved difficult to define grids of acceptable quality for configurations with close-coupled components or complex intersections. Such features are mostly associated with 3-D configurations but an aerofoil and flap is an example of a close-coupled configuration in 2-D and Fig 4(a) shows a multiblock grid about the aft part of such a configuration.

Derivation of this grid involved adjustment of block boundary positions and grid point distributions on block boundaries, using the graphical grid editing facility. However, the grid still leaves something to be desired in terms of detailed cell shape in the gap region, sharp changes in grid density and kinks in grid lines. It is possible that the grid could be further improved but with this type of configuration the final grid quality achieved is likely to depend on geometric features such as flap gap and overlap.

In contrast to the multiblock grid with quadrilateral cells, a grid composed of triangular elements over the gap region of the same configuration is shown in Fig 4(b). The triangles are nearly equilateral and the grid density varies smoothly and is highest where high flow gradients would be expected. Generally, the triangle, the lowest order geometric simplex in 2-D, lends itself naturally to the generation of high quality grids about arbitrary shapes. The attractions of using triangular elements, or tetrahedra in 3-D, for the generation of grids about complex configurations have stimulated investigations by various researchers, eg Refs 13,14. Such grids are referred to as unstructured because neighbouring nodes are, in general, not directly addressable, as is the case with structured grids comprising quadrilaterals, or, in 3-D, hexahedra. At ARA, a new multiblock system is being developed which incorporates certain features of the unstructured grid approach.

A pilot study carried out at Swansea University on behalf of ARA has involved a 2-D investigation of the prospects for incorporating unstructured grids in place of certain blocks within the multiblock grid[15]. Broadly, this approach seeks to introduce the advantages of unstructured grids, such as flexibility in dealing with complex boundaries and ready amenability to grid refinement, where these are most required. Retaining a structured grid over the main part of the flow field offers computational advantages in memory requirements and the full utilisation of the vector capabilities of supercomputers. The advantages of unstructured grids may be introduced in various ways, specifically:

- replace poor quality regions of structured grid by unstructured grid e.g. where negative volume cells occur, or where there are highly stretched/distorted cells near singular points.
- improve the quality of flow prediction by refining a local unstructured grid according to gradients in the flow field.
- introduce extra geometric components with their own structured grid, using unstructured cells at the interface with the overall grid.

In the study, schemes for solution of the Euler equations on hybrid structured/unstructured grids were implemented and these showed that high quality results could be obtained, with little deterioration across interfaces.

In attempting to introduce the hybrid concept in 3-D, a number of factors must be taken into account. For example, consider the subdivision of a hexahedral cell into six tetrahedral cells, as shown in Fig 5(a). This number compares with the subdivision of a quadrilateral cell into only two triangular cells in 2-D. The relatively much larger number of cells required to fill a given volume of space is a factor which leads to a considerable increase in the data storage requirement in 3-D.

Another factor which must be given particular attention in 3-D is the treatment of the interface between the structured and unstructured regions. An appropriate control volume for the finite-volume, cell-vertex solution to the Euler equation for a hybrid grid is readily defined if each face of a cell in the hybrid grid abuts onto one and only one face of another cell. For this purpose, an additional cell shape of pentahedral (pyramid) type is introduced, see Fig 5(b). Incidentally, the subdivisions in Figs 5(a,b) may not be immediately apparent to the eye and this suggests that, although sophisticated graphics facilities will be essential to evaluate such grids, visual effects may still present problems.

In developing the new hybrid structured/unstructured 3-D multiblock system[16], extensive development has been undertaken involving both the grid generation and Euler flow solver components of the system. The data structure involves the unique numbering of each node of the grid and the setting up of connectivity matrices associated with each polygonal face of the pentahedral and tetrahedral elements. The connectivity matrices relate the nodes on a polygonal face to the remaining nodes of the adjacent elements sharing that face. The Euler flow solution[17] is obtained by an extension of Jameson's algorithm[18] in which the control volume is composed, in general, of a combination of hexahedral, pentahedral and tetrahedral volumes, using information derived from the connectivity matrices. Both cell-vertex and cell-centre versions of the scheme have been implemented, enabling a direct comparison of the two formulations to be obtained.

Following the recommendations of the pilot study, the code includes a facility to subdivide an initial structured multiblock mesh into microblocks, of much smaller volume than the original blocks. The microblocks may be evaluated for grid quality and replaced by regions of unstructured grid, if necessary. An algorithm has been developed to accumulate the remaining microblocks into a limited number of macroblocks and enhanced computational efficiency is obtained by vectorisation of the long arrays in the macroblocks. This technique is also applicable to a conventional multiblock grid.

To evaluate the code, solutions have been obtained for various test cases including a channel flow with a bump[16], for which high quality solutions given by other methods are available. The channel flow domain was separated into various regions, and solutions obtained with the alternatives of hexahedral, tetrahedral or pentahedral cells in each region. Broadly it was found that good quality solutions were obtained for all grid types when the finest grid was used but that purely hexahedral cells were preferable with the coarser grids. Also the introduction of unstructured regions resulted in an appreciable increase in the computational memory requirement and reduction in speed of flow solution convergence.

To evaluate the alternative cell-vertex and cell-centre codes, solutions have been obtained for the ONERA M6 wing[19]. Surface pressures at selected stations across this wing given by the two codes using the same grid are shown in Fig 6, compared with experiment. It is difficult to draw conclusions about the accuracy of the solutions due to the absence of viscous modelling from the theory but the quality of shock prediction by the cell-vertex scheme appears the more satisfactory. Note that, despite a somewhat greater computational expense, the cell-vertex code is

preferred, in principle, for the hybrid system, in part because extrapolation techniques which obtain surface flow quantities to satisfy boundary conditions are required of cell-centre schemes and these are more difficult to implement for unstructured grids.

So far, nothing has been said about the means of constructing the grid in the unstructured regions. The approach taken is to use the Delaunay algorithm for automatically connecting points of the grid. This provides a unique set of connections which define, for a given set of points, the most nearly equilateral set of cells over the domain. To define surface grids, a 2-D algorithm[20] has been developed which automatically generates points over the surface which satisfy the Delaunay requirements, given only fixed boundary points. This algorithm was used to generate the grid shown in Fig 4(b). In 3-D, points on the surface and fixed field grid points are connected using the Delaunay algorithm. This includes the introduction of new points where required over the surfaces of the unstructured regions, to ensure that the triangular faces of the cells are consistent with the 3-D Delaunay requirement.

In order to check the viability of the hybrid approach and the quality of solution for 3-D aircraft configurations, multiblock grids have been generated about a wing/body for several cases. Extra geometric components, such as a foreplane, underwing store or engine nacelle are introduced and the structured grid is then deleted in the block(s) where the components are located. Unstructured grids are generated over the surfaces of the extra components and within the block(s). An example of a surface grid defined by this approach for a wing/body/pylon/nacelle configuration is shown in Fig 7.

The optimum approach to the inclusion of regions of unstructured grid in the production version of the system has not yet been finalised but is likely to involve extensive automation to minimise unnecessary or inappropriate user interaction. Also it is envisaged that viscous modelling will be introduced at an early stage, and this will be referred to in section 5.

3 ROTORS

A programme of work in this area has been underway since 1982, involving the development of methods for predicting flows about both conventional and high-speed propellers[3]. The latest developments in this work program will be considered here. Work is also being undertaken on aerofoil design for the unsteady conditions on helicopter rotor blades but this will not be discussed here.

Methods for propeller flow field prediction may be classified into two types, wake and field methods. Wake methods provide a means of determining the onset flow at the blade according to some model of the wake development, and this may be combined with blade element lift and drag data to give radial loading and performance. The field methods provide a description of the complete propeller flow field, including blade pressures and wake development. Methods providing a solution to the Euler equations allow the wake vortex sheets to be captured and are thus felt to represent the minimum standard of modelling complexity acceptable for the complete propeller flow field. However the lack of viscous modelling in such methods is particularly limiting for propeller applications. Together with the significant computational requirement, this means that the wake methods are likely to be used for design and parametric study purposes for many years to come. The Euler methods are used, typically, for detailed investigations, the value of which depends on the quality of the flow solution. This will be discussed here.

For some years the standard Euler code used in the UK for propeller flow field analysis has been a variant of the well-known Denton turbomachinery code[21]. The code provides a solution to the Euler equations in a cylindrical polar coordinate system rotating with the blades, using a cell-vertex, finite-volume technique with a simple multigrid time-stepping scheme. The modifications to the code to make it suitable for use with propellers essentially involve extending the grid outboard of the blade tips and imposing suitable far field boundary conditions. Examples of use of the Denton code for propeller applications are given in Ref 3.

Although the Denton code has proved to be a valuable tool, experience has shown it to have several drawbacks. Firstly, the extra terms introduced into the Euler equations to ensure convergence of the numerical scheme result in excessive dissipation in the solution, smearing shock waves and modifying suction peaks. Secondly, the code is not robust, failing for some cases for no apparent reason. Finally, even with multigrid the code may take several thousand time steps to converge. For these reasons, a second Euler code, referred to as JamProp, has been under development at ARA.

The JamProp code is based on the Jameson cell-centre finite-volume scheme[12] transformed to a rotating Cartesian coordinate system. It uses the now standard convergence acceleration techniques of Runge-Kutta time stepping, rothalpy damping and implicit residual smoothing. A multigrid scheme has also been incorporated but is not yet fully satisfactory. As with the Denton code, an H-type grid between adjacent blades is used, aligned with the helical flow direction but extending further upstream and downstream of the propeller disc plane. The solution is obtained with no-throughflow boundary conditions on the blade surfaces, periodic boundary conditions upstream and downstream of the blades and radial equilibrium at the downstream boundary, as with the Denton solution. Riemann invariant boundary conditions are imposed at the outer boundary, rather than the constant static pressure assumed in the Denton solution, and at the upstream boundary.

One of the problems in developing CFD codes for propellers is that for validation purposes it is necessary to compare the predictions with measurements from tests on pressure - tapped blades but very few suitable experiments of this type have been carried out. One source of high-quality data is the series of tests carried out by NACA in the late 1940s, involving full-scale two-blade propellers of rectangular planform having NACA series 16 aerofoil sections. Comparisons for the NACA 10-(3)(066)-033 propeller[22] are considered here. The grid used for the calculations is shown in Fig 8 , with an infinite parallel sided centrebody assumed.

Pressures at two stations on the blade at a given operating condition are shown in Figs 9 (a,b), comparing experiment with Denton and JamProp results. Pressures are non-dimensionalised by freestream density and onset velocity at a given blade station. The blade geometry used in the calculations includes an approximate representation of the boundary layer displacement surface. Inadequacies in this viscous modelling are the likely cause of differences in pressures between theory and experiment approaching the trailing edge and, possibly, in suction levels ahead of the shock on the upper surface at the outer station. Note that viscous effects on NACA series 16 aerofoil sections are severe in many conditions due to the large included angle at the trailing edge.

The Denton prediction in Fig 9(a) is reasonably close to experiment and may be regarded as a baseline against which to

assess the JamProp prediction in Fig 9(b). The JamProp prediction represents a detailed improvement over Denton particularly in respect of peak suction and shock wave definition. To achieve this standard of prediction, however, it was necessary to introduce a modified, directionally scaled, artificial dissipation model into the method and to increase the grid density normal to the outer blade surface. Without these features the prediction was significantly worse than given by Denton. The JamProp solution was the better converged in that the computational time required for the surface pressures to stabilise was about half that of the Denton solution.

Experience with using the JamProp code for various propeller configurations at various operating conditions has shown that differences in the predicted blade pressures compared with Denton are similar to those in the above example. Also the method is more robust, with convergence to engineering accuracy in far fewer iterations. With both methods the type of grid structure used is not ideal in terms both of radial grid spacing normal to the blades and the fit of the H-type grid to the leading edge profiles. These factors are more significant with conventional than high speed propellers due to the generally lower blade number, smaller ratio of the hub to the tip radii, and bluffer blade aerofoils[2] of the former. Improvements to the grid structure used are not straightforward and will not be considered here.

Aside from the blade characteristics, the development of the propeller wake is of interest. The propeller designer has an interest in the wake model because it is the basis of the strip analysis methods and because the rear rotor of a contra-rotating propeller is immersed in the wake of the front rotor. The aircraft designer has an interest in the wake model because the wake may interact with the flow about the main airframe. Fig 10 shows a special purpose grid used for Denton and JamProp calculations as part of a research investigation into the wake development of an eight-blade high speed propeller. An infinite parallel sided centre body is assumed and the grid extends to a distance of seven blade radii downstream, with a reasonably close spacing of grid lines in order to capture the wake development adequately.

The calculations were performed at a condition M = 0.68 J = 3.0, at which the tip speed was just subsonic. Reasonably well converged solutions were obtained using both codes. Figs 11(a,b) show that blade pressures given by the codes are generally similar although the JamProp results appear more plausible in terms of peak suctions, shock wave definition and smoothness. Figs 12(a,b,c) show calculated wake axial and swirl velocities and pressures, at a station about two blade radii downstream of the disc plane, the values shown being averaged circumferentially and plotted across the radius to the outer boundary. The edge of the wake is indicated by the sharp reduction in velocities towards freestream zero. Over the wake radius the Denton and JamProp velocities compare reasonably closely and it is not clear which are the more correct. Outboard of the edge of the wake the Denton velocities overshoot in an implausible manner. The Denton pressures are also implausible, being wavy and differing from free stream outboard of the edge of the wake. The JamProp pressures rise to a free stream value on moving outboard across the wake, and this would be expected from radial equilibrium considerations, with the dip in the tip region presumably resulting from the presence of the tip vortex.

Overall, it is felt that the JamProp code provides a better prediction of the propeller flow field than does the Denton code. Development of the code is continuing, as required, to extend its applicability and further improve its performance. A by-product of the availability of two very different codes for the solution of the same flow equations is that results for a given configuration and flow condition may be compared directly, giving a better appreciation of the quality of each set of results, as here. This is particularly important in the case of propellers, for which very little detailed experimental flow information of high quality is available.

4 PROPULSION

Work undertaken in the propulsion area has mostly involved the development of codes for the modelling of the flow about aircraft jet propulsion units in isolation. Codes have been developed for calculating the transonic potential flow about both axisymmetric and general 3-D inlet configurations, and for providing viscous-coupled Euler solutions and Navier-Stokes solutions about axisymmetric afterbodies with single or co-axial stream jets. The transonic potential flow inlet code[23] is well established and will not be discussed here. The Euler and Navier-Stokes methods and some examples of their application will be discussed briefly.

Viscous-coupled Euler Methods

Fig13 shows a schematic of an afterbody/nozzle flow field. A method[24] has been developed to predict this flow field by the modification of an inviscid algorithm to include the effects of viscosity on the afterbody surface and in the wake region. In common with methods discussed in previous sections, the Euler algorithm of Ref 12 is used, with the novel feature that the vortex sheet which emanates from the afterbody trailing edge is fitted, rather than captured, as is more widely practised. A representation of viscous effects is included through the calculation of a boundary layer on the external surface of the afterbody and its development into the wake region. This is accomplished using an inverse turbulent boundary layer method[25] and a semi-inverse viscous-inviscid coupling technique[26]. To model the entrainment of fluid from the external region into the jet region, an empirical correlation is incorporated in the method. Results given by this afterbody method will be shown later, compared with results given by Navier-Stokes modelling. Firstly, a recent extension of the method to include the intake flow field will be considered.

Methods which provide either inlet or afterbody flow solutions are suitable for many propulsion applications. However, there is a trend towards higher by-pass ratios for turbofans suitable for transport aircraft, the cowls being of increased radius but reduced length and thus likely to feature an interaction between the intake and afterbody flow fields. The viscous-coupled Euler method has been extended to include the intake flow field, in order to model this interaction[27]. The complete propulsion unit grid, as illustrated below, is generated by combining the grid procedure of the afterbody method[24] with the procedure used in the transonic potential flow method for inlet configurations[23], with modifications to ensure that the grids are compatible. The inviscid flow algorithm remains essentially unchanged apart from the introduction of a new boundary condition to represent flow into the engine face. The inverse turbulent boundary layer method is modified by including a direct laminar boundary layer calculation.

As an example, a cowl profile representative of a short cowl configuration is shown in Fig 14 . A grid generated using the method for the complete unit is shown, together with assumed engine intake and exhaust face positions. Pressures given by the method, assuming a free stream Mach number of 0.9, mass flow ratio of 0.636 and jet pressure ratio of 2.9, are shown in Fig15.

The pressures over the short cowl are compared with those given by a lengthened version of the same geometry derived by inserting an extensive parallel region at the crest position. The pressures on the front portion of the long cowl can be regarded as representative of a forecowl in isolation, as was confirmed in the validation of the method by comparison with calculations by the transonic potential flow inlet code. The comparison in Fig15 demonstrates that the presence of the afterbody has produced a significant effect on surface pressures on the forecowl. Thus use of a method which predicts the complete flow field is likely to be essential for such configurations.

Navier-Stokes Methods

The viscous-coupled Euler codes for the afterbody and complete unit have been released within the UK, providing computationally efficient and generally accurate tools for research and design purposes. However the flow model assumed would not be expected to provide adequate representations of such features as extensive separation and complex mixing regions. Also, the method includes an empirically based parameter to provide a model of the entertainment of fluid from the external region to the jet region and this cannot be regarded as an entirely satisfactory feature of the method. In addressing these problems, an afterbody method involving solution of the Reynolds-averaged Navier-Stokes equations has been developed[28]. In this method, the Navier-Stokes algorithm used is a direct extension of the Euler algorithm used in the viscous-coupled methods. The thin shear layer approximation is invoked and the turbulence models used are either the algebraic model of Baldwin and Lomax[29] or the low Reynolds number form of the k-ε differential model, developed by Chien[30]. The grid spacing in a surface normal direction is much closer to the afterbody and nozzle walls than given by the Euler method grid generation procedure. The run times to produce converged solutions for the Navier-Stokes code are, of course, appreciably longer than for the viscous-coupled Euler code, by a factor of 3-4 in the case of the algebraic model and a factor of 5-6 in the case of the k-ε model.

In general, attached flow cases are predicted equally well by each flow model. For separated flow cases, two examples comparing the performances of the various methods are shown in Figs 16,17. In Fig 16 predicted pressures are compared with experiment for a circular arc afterbody case for which the surface slope is sufficiently steep to provoke separation, as indicated by the plateau in experimental pressures approaching the trailing edge. It can be seen that the viscous/inviscid method gives the better prediction of pressures, using a standard value of the entrainment parameter. In Fig 17 results for a different configuration are shown, for a case where the shock/boundary layer interaction on the conical afterbody is sufficiently strong to cause flow separation. The algebraic model again performs badly but the k-ε model gives a much improved prediction. The viscous-coupled Euler method also gives a reasonably satisfactory prediction of pressures. In both Figs 16 and 17, the predicted separation positions and downstream pressure gradients are not entirely plausible, according to all of the methods used. This is believed to be due to inadequacies in the modelling of the turbulence development as skin friction approaches zero, not surprising in the case of the viscous-coupled Euler method since the skin friction relationship used in the boundary layer method was never intended to apply to such conditions.

In both of these comparisons it was found that results given by the algebraic model could be much improved by introducing a relaxation model for the evaluation of eddy viscosity[31], depending on the value of an empirical parameter governing the rate of relaxation. However, this degree of empiricism was felt to be unacceptable in a method which is intended to provide a general capability. Generally, it is felt that the Navier-Stokes method with the algebraic turbulence model offers little or no improvement over the viscous-coupled Euler method, with a considerable computational penalty. The Navier-Stokes method with the k-ε turbulence model, which can additionally deal with thick trailing edges, requires further development. Such development work is being undertaken at ARA, including investigation of higher-order (Reynolds' stress) turbulence models.

5 VISCOUS FLOWS

The multiblock system for grid generation and Euler flow solution about complex configurations, discussed in section 2, provides a substantial advance over earlier methods in the levels of geometric and flow complexity which can be dealt with. However, the lack of viscous modelling limits the accuracy of prediction and range of applicability of such methods. Hence, the current multiblock work programme includes the introduction of Navier-Stokes modelling into the new hybrid structured/unstructured multiblock system. As a precursor to the 3-D work, an exercise involving 2-D Navier-Stokes modelling with unstructured grids has been carried out [32] and some of the issues arising will be considered.

Other work on viscous flows has included further development of the BVGK method[33] for prediction of the viscous-coupled compressible potential flow about an aerofoil. This is an established method in widespread production use within the UK. Part of the work at ARA has involved investigation of the modelling of extensively separated flow regions and this will be discussed here briefly. Work is also being carried out on higher-order turbulence modelling of aerofoil flows but this will not be discussed here.

Viscous Modelling With Hybrid Grids

The first stage of this investigation involved the development of a method to provide a solution to the Reynolds-averaged Navier-Stokes equations on unstructured triangular grids. In this method, the governing equations are discretised using a finite-volume, cell-vertex algorithm due to Jameson[18]. Use of a cell-vertex algorithm is consistent with the preferred approach for the new, hybrid structured/unstructured multiblock system, see section 2.

In obtaining a numerical solution to the equations it is necessary to introduce artificial dissipative terms, to ensure stability of convergence and the adequate capture of singularities such as shock waves in the inviscid regions of the flow field. Thus it is important to examine at the outset the inviscid solution, to ensure that the effects of artificial dissipation are not excessive with the typical grids required for the viscous solution. This will be considered in the following example.

Fig 18(a) shows a Delaunay grid about an RAE 2822 aerofoil, generated using the method of Ref 20. The grid extends to a circular far field boundary at a distance of about 11 chord lengths from the aerofoil and contains about 2,000 points. Fig 18(b) shows the same overall grid with increased density local to and normal to the surface, going some way towards the type of grid required for a viscous calculation. This grid contains about

3,000 points. Note that the cells close to the surface are directly triangulated from quadrilateral cells. It was not appropriate to generate the grid in this region using the same Delaunay algorithm as for the overall grid, since it forces triangles to be as nearly equilateral as possible and so very close point spacing along the surface would have been needed to give the required grid density in a direction normal to the surface, resulting in an excessive total number of grid points.

Flow calculations using the Navier-Stokes code in Euler mode were performed for the RAE 2822 aerofoil with the two grids at $M = 0.73$ $\alpha = 2.79°$, Case 9 of Ref. 34, and the results are shown in Figs 19(a),(b). The solution using the Delaunay grid is believed to be of reasonably high quality, with the change in entropy levels through the shock approximately consistent with the Rankine-Hugoniot shock jump (indicated by RH). In contrast, the inclusion of the directly-triangulated grid region has produced a poor quality solution, with unrealistic local Mach number and entropy levels downstream of the shock. Even so, this poor quality solution was an improvement on an earlier solution, the improvement being achieved by introducing directional scaling into the artificial dissipation terms to take some account of the orientation of the high aspect ratio cells close to the surface. The high aspect ratio of these cells is believed to be the main reason for the poor quality of solution.

For viscous calculations it was found possible to reduce the magnitude of the artificial dissipation and thus improve solution quality by scaling normal components by a function of the ratio of local to free-stream Mach number, with the real dissipation sufficient to stabilise the numerical solution. Examples of such calculations included a flat plate laminar flow case for a Mach number of 0.8 and Reynolds number of 5000. A directly triangulated grid close to the surface was used, corresponding to that used by Mavriplis et al[35] for the same problem, and the flow solution precisely matched the exact Blasius solution. Also a turbulent flow solution was obtained for the RAE 2822 aerofoil case 9 using the Baldwin-Lomax turbulence model[29], again with a directly triangulated grid close to the surface, and was found to be of comparable quality to solutions for this case obtained elsewhere.

The code has been extended to include regions of both structured quadrilateral and unstructured triangular grid. Fig 20 shows an example of a grid of this type about a NACA 0012 aerofoil. It has been found that the flow solution is typically of comparable quality to that using a fully quadrilateral or fully-triangulated grid as long as the cell volume does not change abruptly on moving across a boundary between quadrilateral and triangular regions. This is ensured by extending the quadrilateral region well away from the aerofoil surface and introducing the 'fish tail' effect, as shown. Thus there appears to be little need to introduce direct triangulation of structured grids, particularly bearing in mind the computational penalties to be expected.

It is likely that grids suitable for viscous multiblock calculations will initially comprise structured grid regions adjacent to the surfaces. This is because it is desirable to introduce directional information into the artificial dissipation terms and because the Baldwin-Lomax turbulence model is likely to be used initially and this requires information on grid lines normal to the surface. It is not straightforward to obtain such information with unstructured grids. However, it is likely that in the longer term it will be necessary to calculate viscous flows using fully unstructured grids which extend down to the surfaces of some complex geometries. This problem is under investigation.

Viscous-Coupled Potential Flow Method

The BVGK code[33] is widely used within the UK for the calculation of transonic flows about aerofoils. The method was developed at RAE but investigations leading to further development have been carried out at ARA, in collaboration with the method developers. The method provides a solution to the compressible potential flow equation in the overall flow field, matched to the viscous flow development on the aerofoil surfaces and in the wake by a viscous/inviscid coupling procedure[36]. An inverse integral boundary layer method[25] is used for the calculation of the turbulent viscous layers. The boundary layer and wake development is represented by a surface transpiration condition in the calculation of the overall flow field. The use of an inverse boundary layer method allows a solution to be obtained in separated as well as attached flow conditions, the method incorporating certain features to improve the turbulence modelling as separation is approached.

As discussed in Ref 33, the development of BVGK included extensive validation against high quality experimental data. The method has been shown to provide accurate flow predictions for a wide range of aerofoil geometries and flow conditions. As an example, the flow development on an RAE 5234 aerofoil is shown in Fig 21. This is a relatively advanced aerofoil, described in Ref. 33, which features an isentropic supercritical recompression to a weak shock and a predicted localised separation at the trailing edge on the upper surface in the condition shown. It can be seen that predicted surface pressures, force and moment coefficients compare closely with experiment. This result is typical of the standard of prediction for cases with attached flows or limited regions of flow separation.

For cases with extensive regions of flow separation (> 10% of the chord, say) it has been found that problems can occur with the numerical scheme. The method tends to predict chordwise oscillations in pressures and boundary layer parameters in such regions. This tendency was particularly apparent for aerofoil RAE 2822 at $M = 0.753$ $C_L = 0.4$, Case 10 of Ref. 34, which features extensive flow separation downstream of the shock on the upper surface. Recent work at ARA has included investigations of ways of resolving this problem.

Fig 22(a) shows pressures predicted by BVGK on aerofoil RAE 2822 at the above condition, compared with experiment, and Fig 22(b) shows the corresponding upper surface boundary layer displacement thickness development. It can be seen that severe chordwise oscillations in both pressures and displacement thickness downstream of the shock occur but are largely removed when a modified version of the code is used. Before the solution to the problem was found, attempts were made to improve matters by direct smoothing of the boundary layer displacement thickness but they were unsuccessful since inconsistencies were introduced into the viscous/inviscid matching. Alternative viscous/inviscid coupling procedures were also investigated[26] but these had little effect. Eventually, it was found that simply switching from upwind to central differences for the displacement thickness slope definition over the separated region in the inverse boundary layer calculation was sufficient to achieve the improvement shown. The modification was also found to provide a substantial improvement in solution convergence characteristics.

Although use of the modified version of BVGK has largely removed the problem with predicted flow oscillations in extensively separated regions, it can be seen from Fig 22(a) that the results for Case 10 still differ significantly from experiment on the upper surface in respect of leading edge peak suctions and

suction levels towards the trailing edge. However, these deficiencies are characteristic of results given by many other methods for this difficult test case, as reported in Ref 37. The reasons for these deficiencies are not known but it is possible that, for example, improvements in turbulence modelling in the shock/boundary layer interaction region would give a better prediction of suction levels downstream of the shock.

Considerable development work is usually required to bring a code from research to production status, involving the introduction of improvements resulting from validation and continual interaction between the developer and the user. The above example demonstrates that it is necessary to continue with such development work even for established codes. Generally, evaluation/development work is regarded as an important part of CFD activity at ARA.

6 CONCLUDING REMARKS AND FUTURE PLANS

The preceding discussion has highlighted recent and current items of research in the field of CFD at the Aircraft Research Association. These items may be summarised as follows:

1. Following the successful development of the ARA multiblock system, the new, hybrid, multiblock system with regions of unstructured grid should provide further advances in both solution flexibility and the geometric complexity of the configurations which can be handled.
2. An Euler code has been developed which provides a better prediction of a propeller flow field than does the extended version of the Denton turbo-machinery code which is used within the UK for this purpose.
3. A comprehensive set of computer codes has been developed for predicting flows about axisymmetric jet propulsion units in isolation.
4. A 2-D investigation into viscous modelling with hybrid grids has provided an appreciation of some of the issues which will need to be addressed in introducing viscous modelling into the hybrid multiblock system.

In addition to the development of new methods, the application, evaluation and development of existing methods is seen as an important part of CFD activity. An example of this is the work on the BVGK code, described here.

Future plans include a continuation of current work items with the following near-term objectives.

- Obtain flow solutions for 3-D complex configurations with hybrid structured/unstructured grids.
- Introduce Navier-Stokes modelling into the hybrid multiblock system and obtain viscous flow wing solutions.
- Introduce improvements in turbulence modelling of flows about, for example, propulsion units and aerofoils.

Other areas of planned future work include 3-D propulsion modelling, propeller/rotor modelling, and transition prediction. The general interest in 3-D flow modelling means that the multiblock grid generation and flow solution capability in its original or hybrid form will become increasingly relevant to many other areas of CFD activity. Although not discussed here, the development of computational facilities, including graphics and pre-and post-processing, is an essential feature of CFD which will receive increasing emphasis.

ACKNOWLEDGEMENTS

The author wishes to thank colleagues at ARA for the information contributed and for their assistance in preparing and checking this paper.

The development of the multiblock system and the work on propulsion and viscous flows described here has been carried out under contract to the Procurement Executive, UK Ministry of Defence. The development of the original, structured, Multiblock system also received partial support from BAe plc. The development of the Euler code for propeller flows has been carried out under contract to Dowty Rotol Ltd.

REFERENCES

1. T J Baker, C R Forsey, A Fast Algorithm for the Calculation of Transonic Flow over Wing/Body Combinations, AIAA Journal, Vol 21 No. 1 pp 60 -67, 1983

2. A J Bocci, A New Series of Aerofoil Sections Suitable for Aircraft Propellers, Aeronautical Quarterly, Vol 28, 1977.

3. P W C Wong, M Maina, C R Forsey, A J Bocci, Single and Contra-rotation High Speed Propellers: Flow Calculation and Performance Prediction, ICAS -88-2.4.2, 1988.

4. J A Shaw, J M Georgala, N P Weatherill, The Construction of Component Adaptive Grids for Aerodynamic Geometries in Computational Fluid Mechanics '88 Edited by S Sengupta, J Hauser, P R Eiseman, J F Thompson, Pineridge Press, 1988.

5. A J Baxendale, Application of a Multiblock CFD Code to Obtaining Flow Field Predictions About Wing/Body/Pylon/Store Configurations, ICAS 90 - 6.6.2, 1990.

6. J L Fulker, P R Ashill, A Theoretical and Experimental Evaluation of a Numerical Method for Calculating Supersonic Flows over Wing/Body Configurations, AGARD - CP - 437 Vol.1 Paper 12, 1988.

7. S E Allwright, Multiblock Topology Specification and Grid Generation for Complete Aircraft Configurations, AGARD - CP - 464 Paper 11, 1989.

8. N P Weatherill, C R Forsey, Grid Generation and Flow Calculations for Aircraft Geometries, Journal of Aircraft ,Vol. 22 No. 10 pp 855 - 860, 1985.

9. R H Doe, T W Brown, A Pagano, The Development of Practical Euler Methods for Aerodynamic Design, ICAS - 86 - 1.4.2,1986.

10. J F Thompson, F C Thames, C W Mastin, Automatic Numerical Generation of Body-Fitted Curvilinear Coordinate System for Field Containing any Number of Arbitrary Two-Dimensional Bodies, Journal of Computational Physics, Vol 15, 1974.

11. J M Georgala, J A Shaw, A Discussion on Issues Relating to Multiblock Grid Generation, AGARD - CP - 464 Paper 16, 1989.

12 . A Jameson, W Schmidt, E Turkel, Numerical Solutions of the Euler Equations by Finite Volume Methods using Runge-Kutta Time-Stepping Schemes, AIAA 81 - 1259, 1981.

13. T J Baker, Unstructured Mesh Generation by a Generalised Delaunay Algorithm, AGARD - CP - 464 Paper 20, 1989.

14. J Peraire, M Vahdati, K Morgan, O C Zienkiewicz, Adaptive Remeshing for Compressible Flow Computations, Journal of Computational Physics, Vol 72 No 2, 1987.

15. N P Weatherill, On the Combination of Structured-Unstructured Meshes, in Numerical Grid Generation in Computational Fluid Mechanics '88, Edited by S Sengupta, J Hauser, P R Eiseman, J F Thompson, Pineridge Press, 1988.

16. J A Shaw, A J Peace, N P Weatherill, A Three-Dimensional Hybrid Structured-Unstructured Method: Motivation, Basic Approach and Initial Results, Proceedings of GAMNI/SMAI-IMA Conference on Computational Aeronautical Fluid Dynamics, Antibes, France, 1989.

17. A J Peace, J A Shaw, The Modelling of Aerodynamic Flows by Solution of the Euler Equations on Mixed Polyhedral Grids, ARA Report in preparation.

18. A Jameson, T J Baker, N P Weatherill, Calculation of Inviscid Transonic Flow over a Complete Aircraft, AIAA 86-0103, 1986.

19. V Shmitt, F Charpin, Pressure Distributions on the ONERA - M6 - Wing at Transonic Mach Numbers, AGARD-AR-138, Paper B1, 1979.

20. P N Childs, Generation of Unstructured Grids Using the Delaunay Triangulation, ARA Memo, in preparation.

21. J D Denton, The Calculation of Fully Three-Dimensional Flow Through Any Type of Turbomachinery Blade Row, AGARD-LS-140, 1985.

22. J D Maynard, M P Murphy, Pressure Distributions on the Blade Sections of the NACA 10-(3)(066)-033 Propeller under Operating Conditions, NACA RM L9L23, 1950.

23. A J Peace, Transonic Flow Calculations around Isolated Inlet Configurations, The Aeronautical Journal of the Royal Aeronautical Society, Vol. 90 No. 893, 1986.

24. A J Peace, A method for Calculating Axisymmetric Afterbody Flows, AIAA Journal of Propulsion and Power, Vol 3 No 4, 1987.

25. L F East, P D Smith, P J Merryman, Prediction of the Development of Separated Turbulent Boundary Layers, by the Lag-Entrainment Method, RAE TR77046, 1977.

26. B R Williams, The Prediction of Separated Flow using a Viscous-Inviscid Interaction Method, ICAS - 84-2.03.3, 1984.

27. L A Sykes, A J Peace, A Viscous/Inviscid Method for the Flow about a Complete Axisymmetric Propulsion Unit, ARA Memo 314, 1989.

28. A J Peace, Turbulent Flow Predictions for Afterbody/Nozzle Geometries Including Base Effects. AIAA Journal of Propulsion and Power, to appear. See also AIAA 89-1865,1989.

29. B Baldwin, H Lomax, Thin Layer Approximation and Algebraic Model for Separated Turbulent Flows, AIAA-78-257, 1978.

30. K - Y Chien, Predictions of Channel and Boundary Layer Flows with a Low-Reynolds-Number Turbulence Model, AIAA Jounal, Vol 20 No.1 pp 33-38, 1982.

31. J S Shang, W L Hankey, Numerical Solution for Supersonic Turbulent Flow over a Compression Ramp, AIAA Journal Vol 13 No.10 pp 1368 - 1374, 1975.

32. L A Sykes, Development of a Two-Dimensional Navier-Stokes Algorithm for Unstructured Triangular Grids, ARA Report in preparation.

33. P R Ashill, Calculation and Measurement of Transonic Flows over Aerofoils with Novel Rear Sections, ICAS-88-3.10.2,1988.

34. P H Cook, M A McDonald, M C P Firmin, Aerofoil RAE 2822 - Pressure Distributions and Boundary Layer and Wake measurements, AGARD-AR-138, Paper A6, 1979.

35. D J Mavriplis, A Jameson, L Martinelli, Multigrid Solution of the Navier-Stokes Equations on Triangular Meshes, AIAA-89-0120, 1989.

35. J E Carter, A New Boundary Layer Inviscid Iteration Technique for Separated Flows, AIAA 70 - 1450, 1979.

37. T L Holst, Viscous Transonic Aerofoil Workshop Compendium of Results, AIAA-87-1460, 1987.

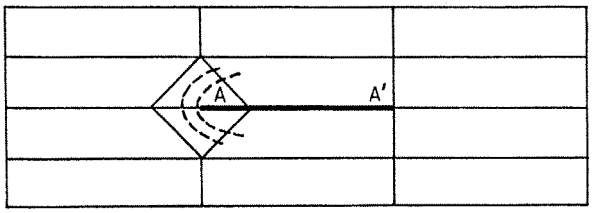

FIG 1(a) C-GRID BLOCK STRUCTURE

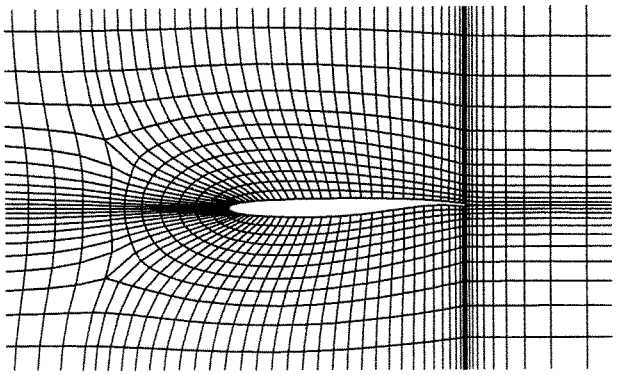

FIG 1(b) C-GRID ABOUT AEROFOIL

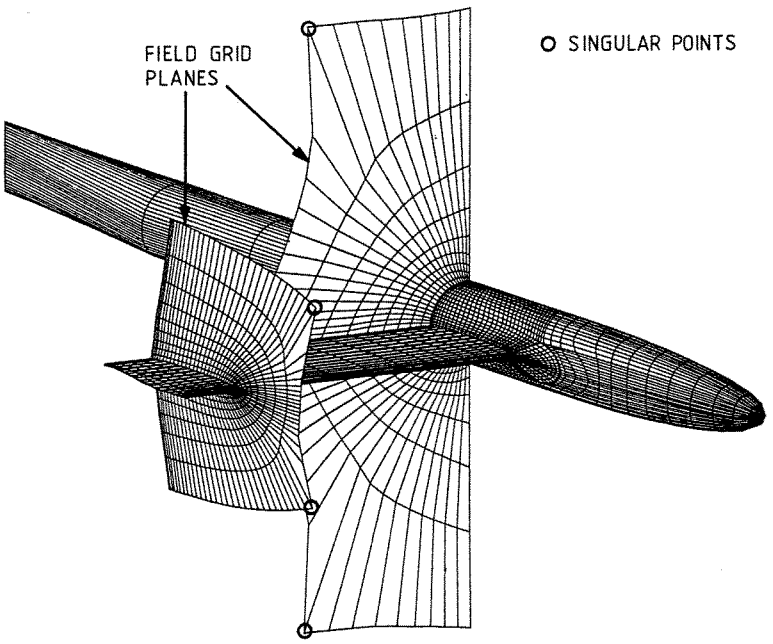

FIG 2 WING/BODY SURFACE GRID AND PLANES THROUGH FIELD GRID

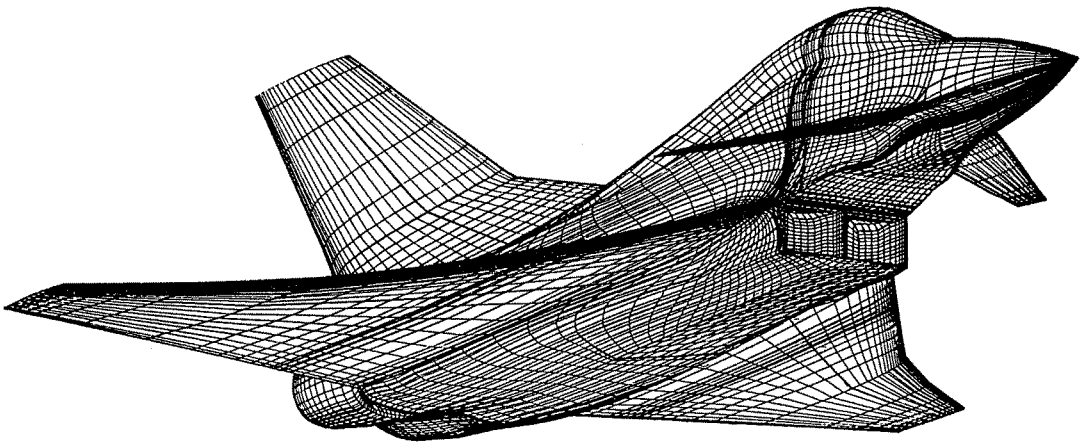

FIG 3(a) SURFACE GRID ON MILITARY AIRCRAFT

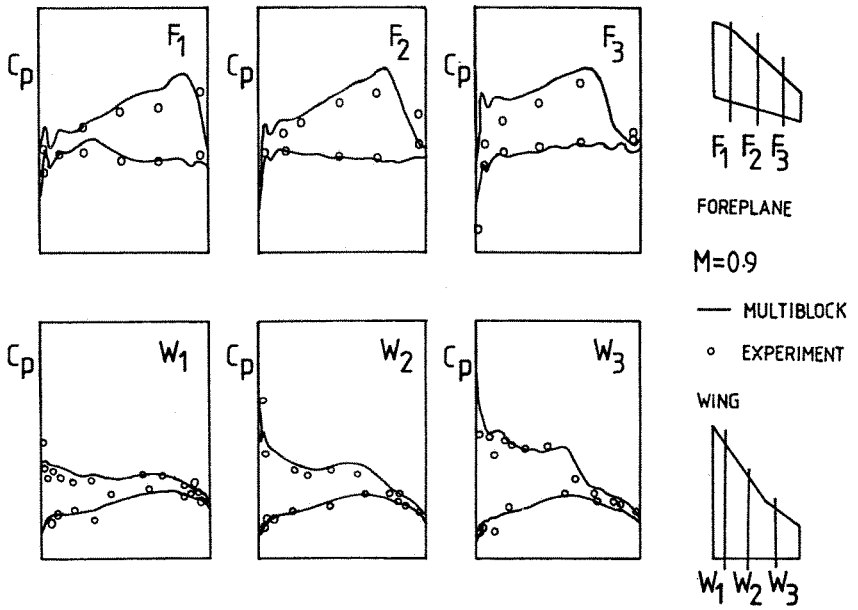

FIG 3(b) PRESSURES ON WING AND FOREPLANE OF MILITARY AIRCRAFT

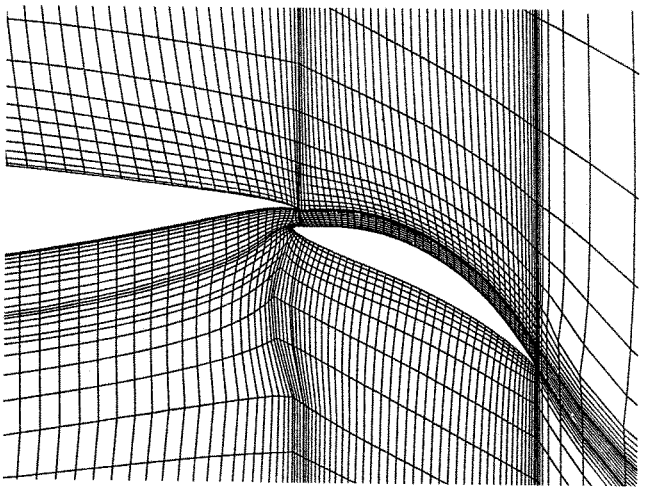

FIG 4(a) AEROFOIL/FLAP MULTIBLOCK GRID

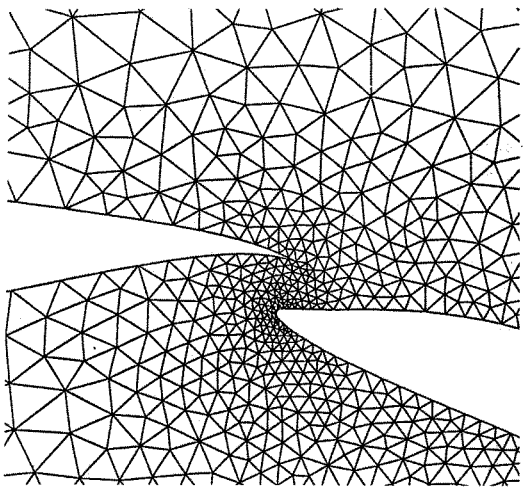

FIG 4(b) AEROFOIL/FLAP GAP REGION, UNSTRUCTURED GRID

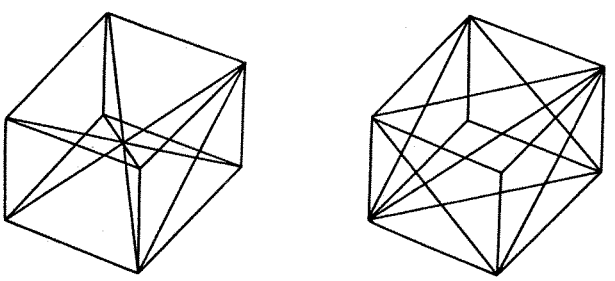

(a) TETRAHEDRA (b) PENTAHEDRA + TETRAHEDRA

FIG 5 DECOMPOSITION OF HEXAHEDRAL CELL

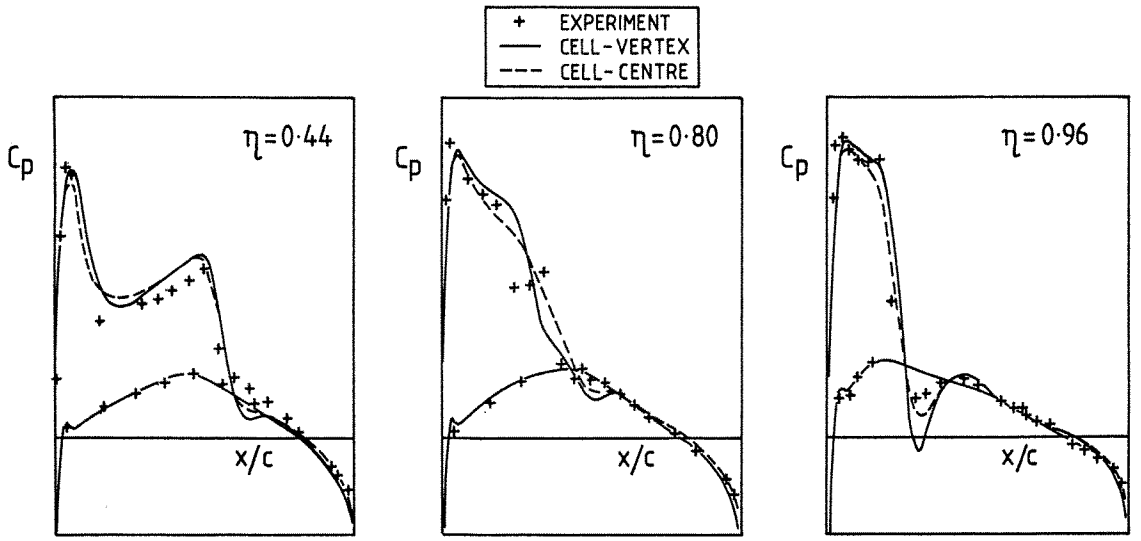

FIG 6 PRESSURES ON ONERA M6 WING M = 0.84 $\alpha = 3.0°$

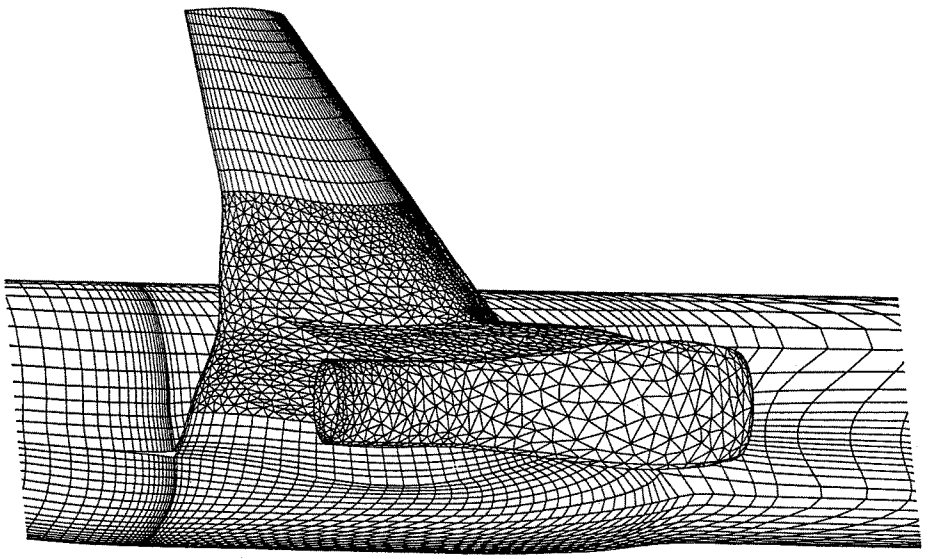

FIG 7 HYBRID SURFACE GRID, WING/BODY/PYLON/NACELLE

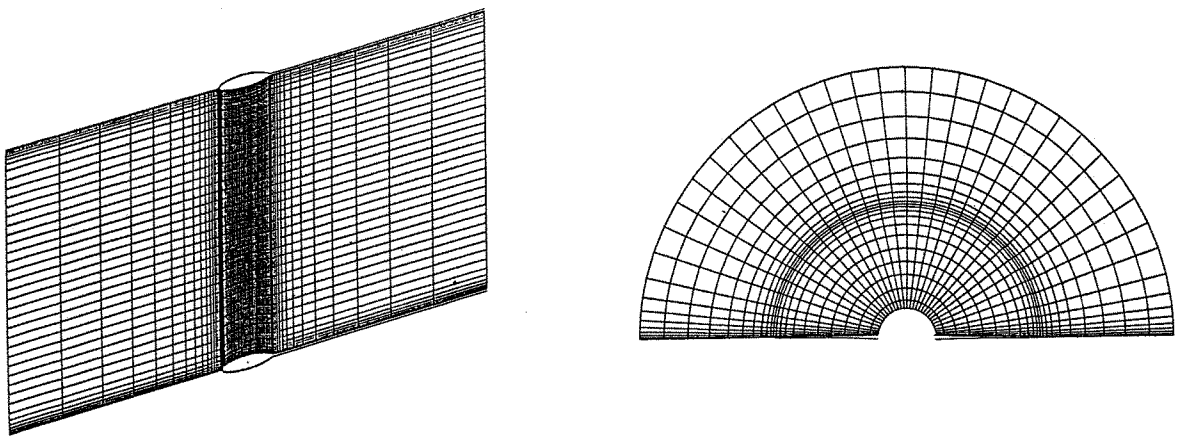

FIG 8 GRID FOR NACA 2-BLADE PROPELLER

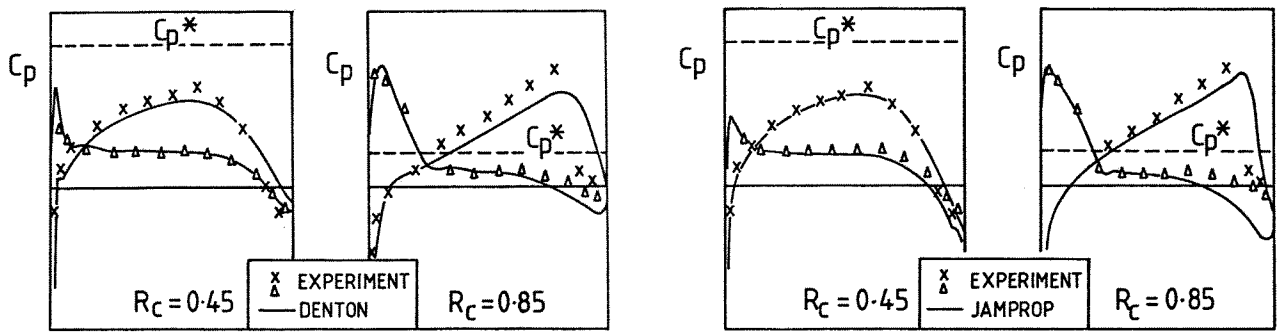

(a) DENTON ~ EXPERIMENT

(b) JAMPROP ~ EXPERIMENT

FIG 9 PRESSURES ON NACA 2-BLADE PROPELLER

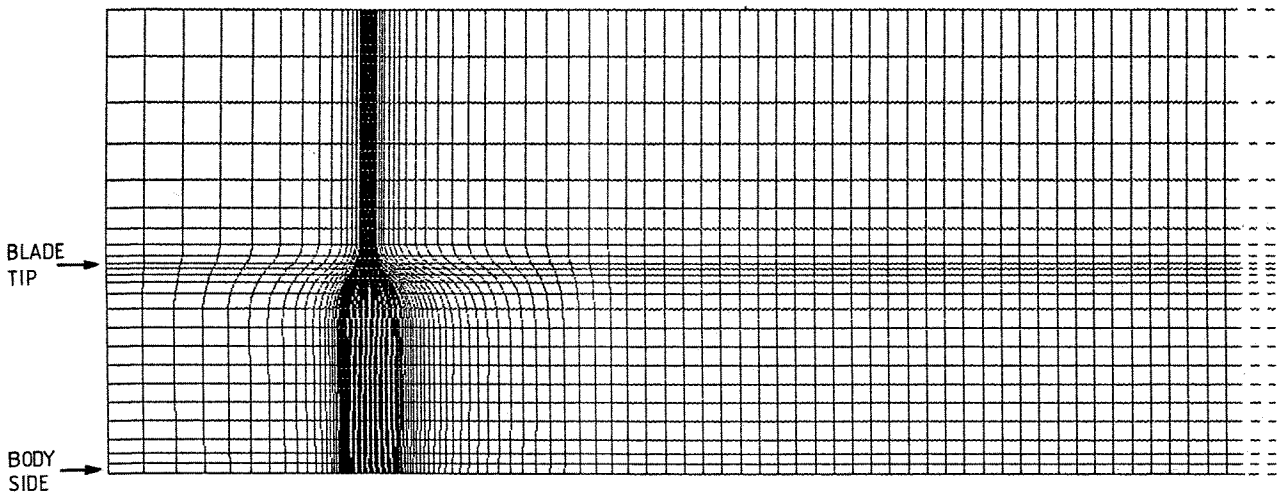

FIG 10 GRID FOR 8-BLADE PROPELLER

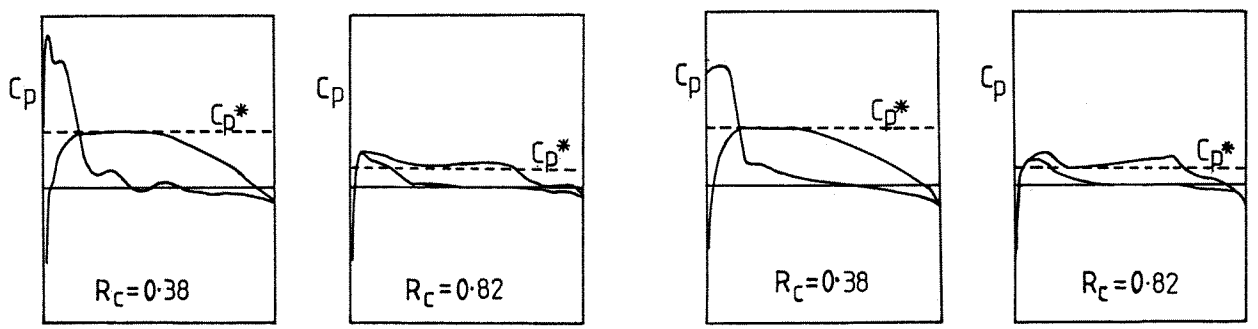

(a) DENTON

(b) JAMPROP

FIG 11 PRESSURES ON 8-BLADE PROPELLER

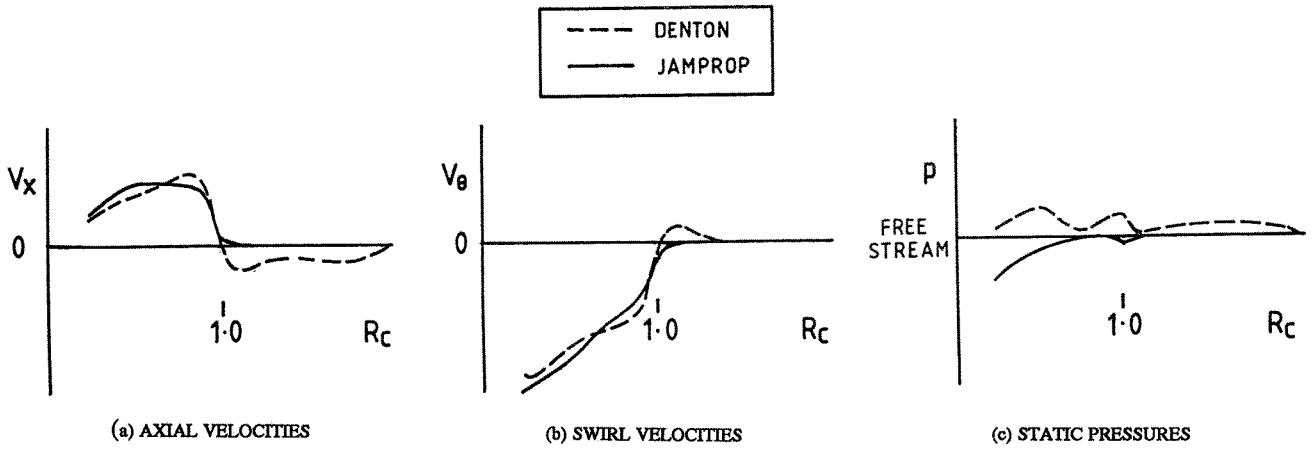

(a) AXIAL VELOCITIES (b) SWIRL VELOCITIES (c) STATIC PRESSURES

FIG 12 WAKE FLOW PARAMETERS, 8-BLADE PROPELLER

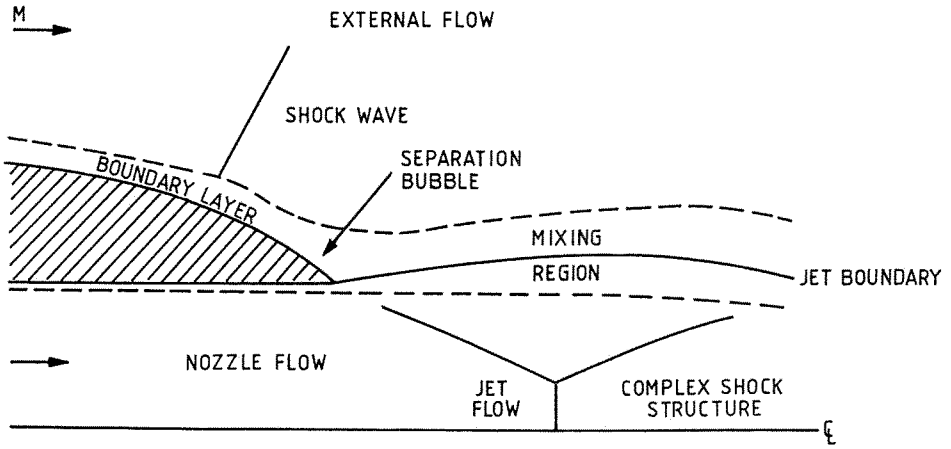

FIG 13 SCHEMATIC OF AFTERBODY/NOZZLE FLOWFIELD

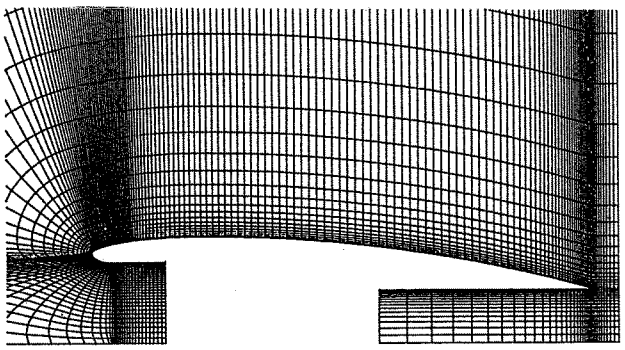

FIG 14 SHORT COWL GEOMETRY AND GRID

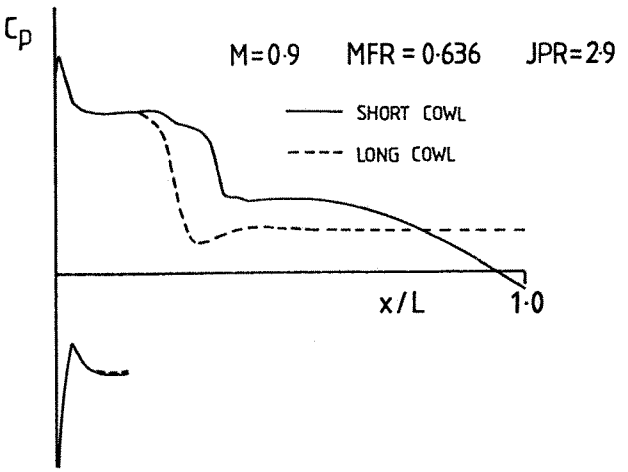

FIG 15 PRESSURES ON SHORT AND LONG COWLS

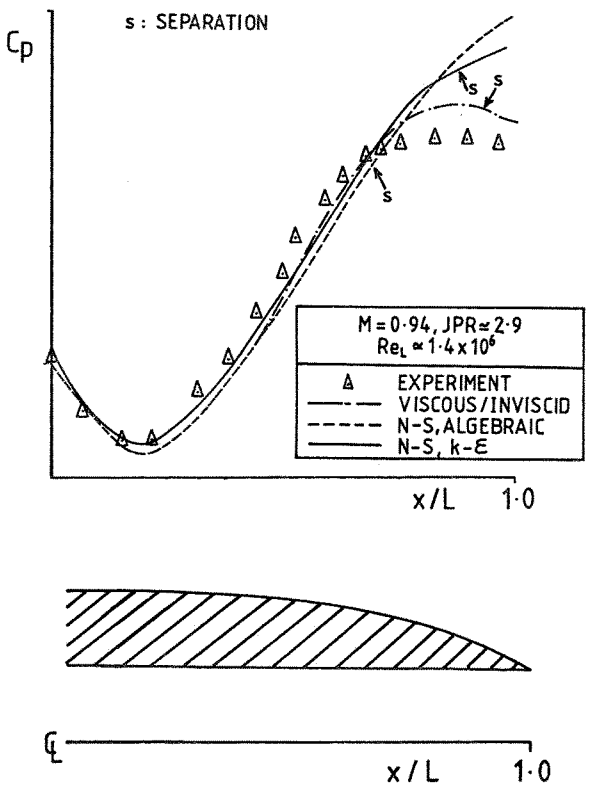

FIG 16 CIRCULAR ARC AFTERBODY, GEOMETRY AND PRESSURES

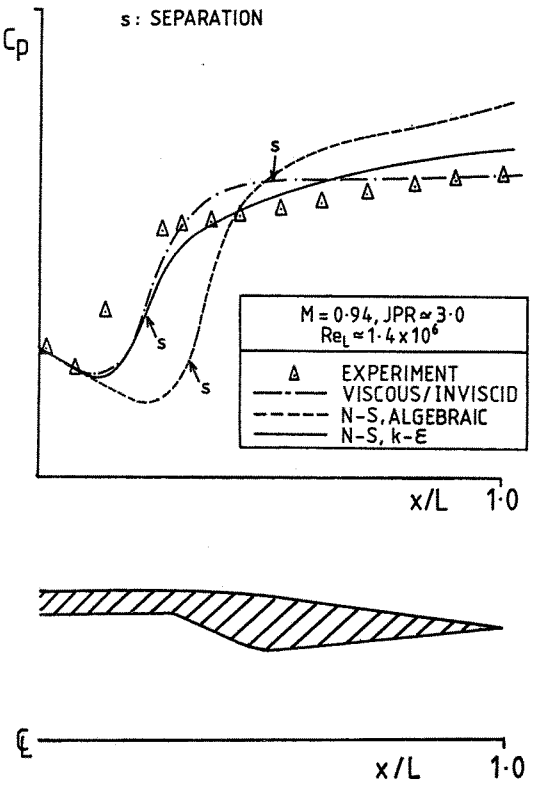

FIG 17 CONICAL AFTERBODY GEOMETRY AND PRESSURES

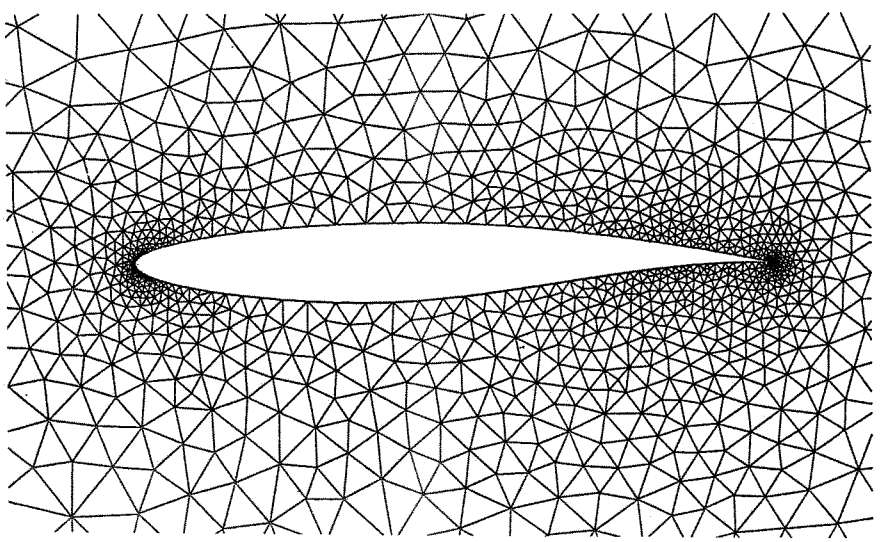

FIG 18(a) DELAUNAY GRID FOR RAE 2822 AEROFOIL

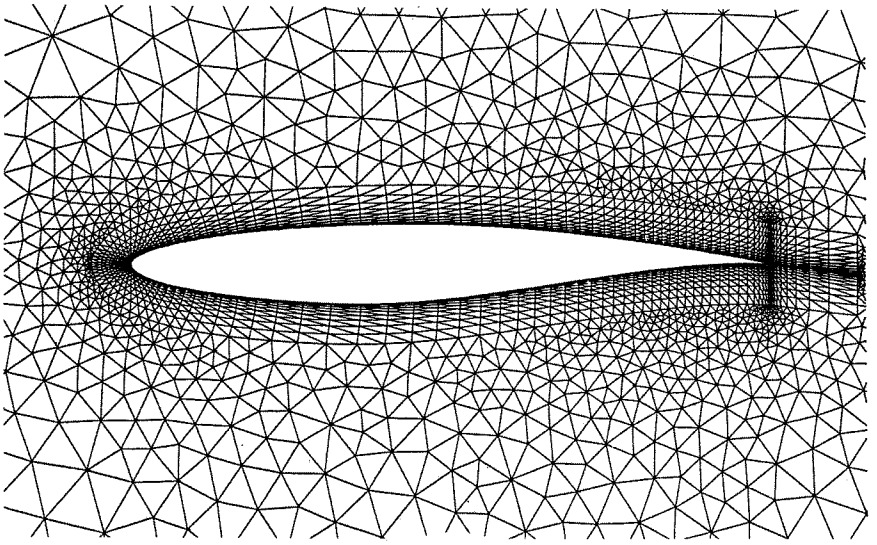

FIG 18(b) DELAUNAY GRID DIRECTLY TRIANGULATED NEAR SURFACE OF RAE 2822 AEROFOIL

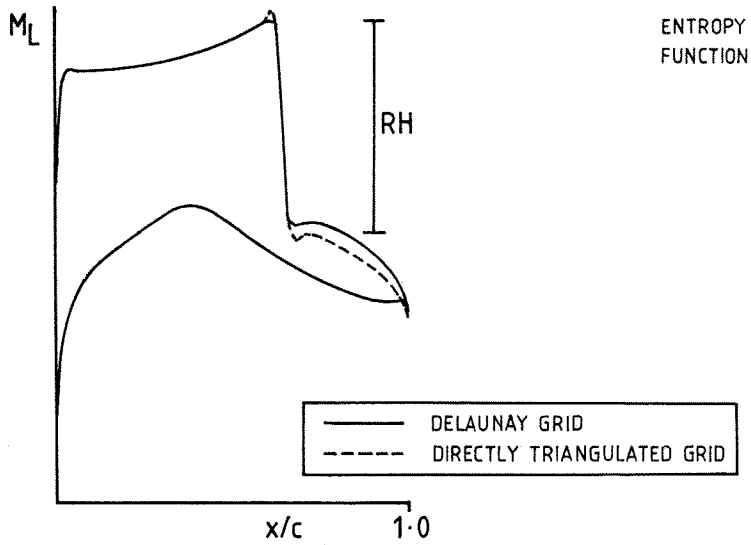

FIG 19(a) LOCAL MACH NUMBERS RAE 2822, AEROFOIL M = 0.73 α = 2.79°

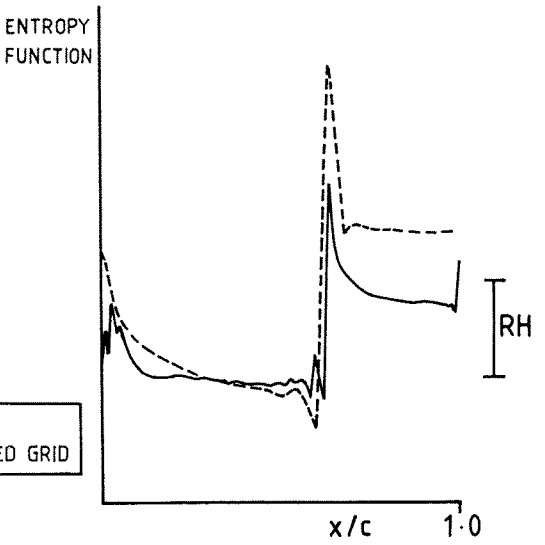

FIG 19(b) ENTROPY FUNCTION, RAE 2822 AEROFOIL M = 0.73 α = 2.79°

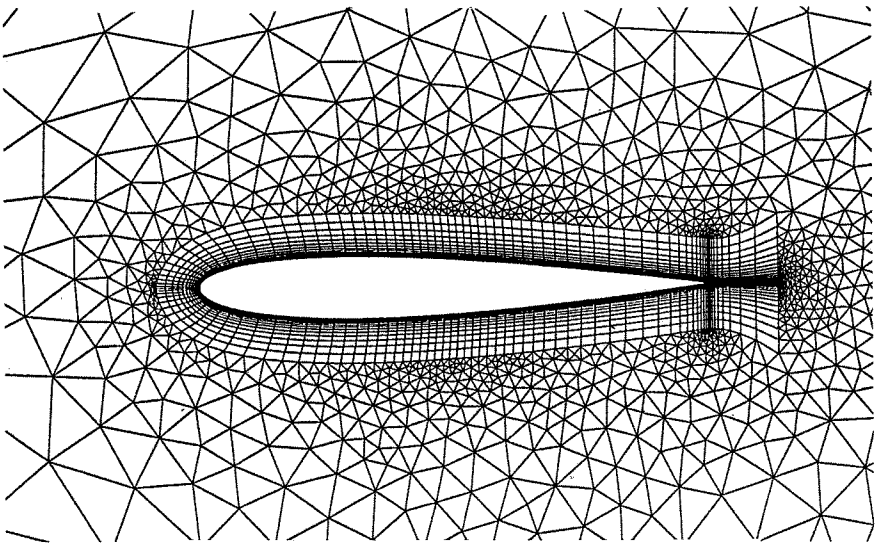

FIG 20 HYBRID GRID FOR NACA 0012 AEROFOIL

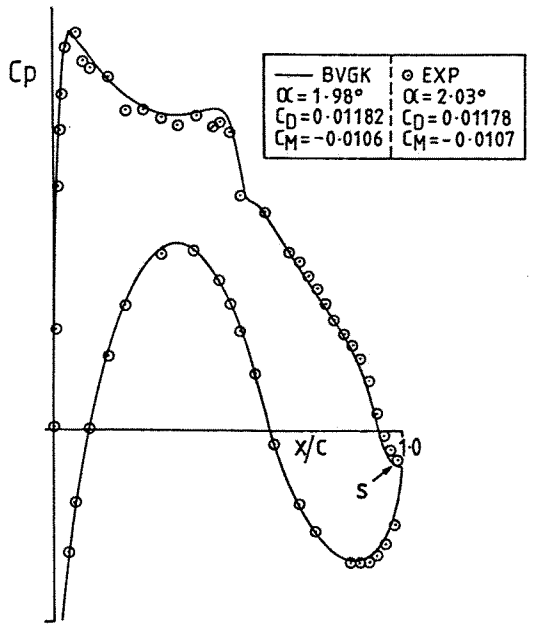

FIG 21 PRESSURES ON RAE 5234 AEROFOIL
$M = 0.736$ $C_L = 0.61$ $Re_c = 6.0 \times 10^6$

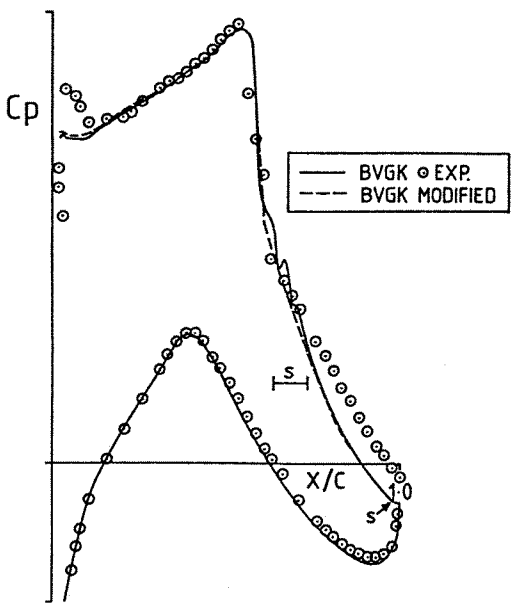

FIG 22(a) PRESSURES ON RAE 2822 AEROFOIL
$M = 0.753$ $C_L \approx 0.74$ $Re_c = 6.2 \times 10^6$

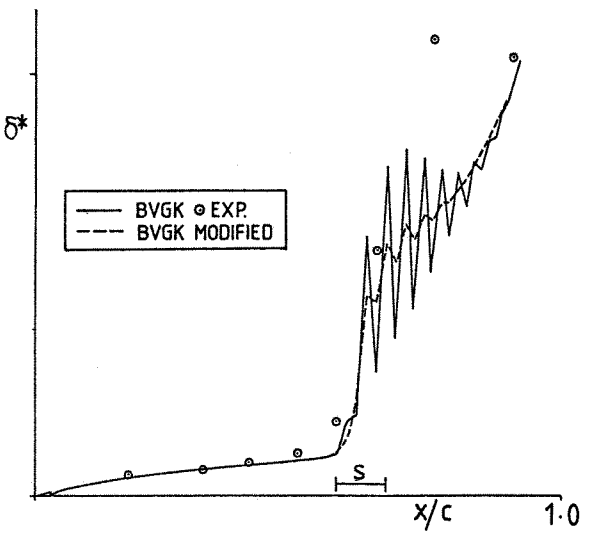

FIG 22(b) DISPLACEMENT THICKNESS DISTRIBUTION ON UPPER SURFACE OF RAE 2822 AEROFOIL
$M = 0.753$ $CL \approx 0.74$ $Re_c = 6.2 \times 10^6$